

Investigation of structural changes in the phase transformations of $\gamma\text{-Bi}_2\text{MoO}_6$

This article has been downloaded from IOPscience. Please scroll down to see the full text article.

2002 J. Phys.: Condens. Matter 14 4001

(<http://iopscience.iop.org/0953-8984/14/15/314>)

View [the table of contents for this issue](#), or go to the [journal homepage](#) for more

Download details:

IP Address: 171.66.16.104

The article was downloaded on 18/05/2010 at 06:28

Please note that [terms and conditions apply](#).

Investigation of structural changes in the phase transformations of γ -Bi₂MoO₆

Ramaswamy Murugan^{1,3}, Raje Gangadharan¹, Jayaraman Kalaiselvi¹,
Shajina Sukumar², Balan Palanivel¹ and Sriramulu Mohan²

¹ Department of Physics, Pondicherry Engineering College, Pondicherry 605 014, India

² Raman School of Physics, Pondicherry University, Pondicherry 605 014, India

Received 5 February 2002

Published 4 April 2002

Online at stacks.iop.org/JPhysCM/14/4001

Abstract

In this work, extensive thermo-Raman investigations have been carried out on a γ (L)-Bi₂MoO₆ sample ('L' indicating the low-temperature polymorph) in an effort to gain an understanding of the structural evolution and phase transformation involved during a dynamical thermal process. The room temperature Raman spectrum of the γ (L)-Bi₂MoO₆ phase indicated the presence of corner-sharing distorted MoO₆ octahedra. The spectral variations, shift in the band positions, decrease in intensities and broadening of the Mo–O modes observed in the thermo-Raman spectra and the thermal evolution of the Mo–O bonds in the temperature interval from 25 to 610 °C strongly suggest that the transformation from the γ (L)-Bi₂MoO₆ to the γ (I)-Bi₂MoO₆ phase ('I' indicating the intermediate-temperature polymorph) involves a gradual anisotropic thermal response of Mo–O bonds initially, upon heating, and further appreciable increase in the octahedral distortion from 310 °C onwards—until the structure is on the verge of becoming composed of distorted tetrahedra. The spectral variation in the thermo-Raman spectra observed for the transformations to γ (H)-Bi₂MoO₆ ('H' indicating the high-temperature polymorph) starting at around 620 °C and ending at 660 °C revealed the sluggish nature of the transformations and also clearly indicated the transformation from highly distorted MoO₆ octahedra to distorted tetrahedra. The comparison of the profile of the Raman spectrum of the γ (H)-Bi₂MoO₆ phase measured at 720 °C and that measured after cooling down to 25 °C clearly rules out the possibility of the formation of a β -Bi₂Mo₂O₉ phase structure consisting of Mo⁶⁺ in tetrahedral coordination at high temperature.

³ Author to whom any correspondence should be addressed.

1. Introduction

Bismuth molybdates, represented stoichiometrically as $\text{Bi}_2\text{O}_3 \cdot n\text{MoO}_3$, fall into an unusual category of compounds, the ternary bismuth oxide systems, Bi-M-O (where $\text{M} = \text{Mo}, \text{W}, \text{V}, \text{Nb}$ and Ta) and they all exhibit interesting physical properties. Bismuth molybdates figure prominently in industry as heterogeneous catalysts in reactions such as selective oxidation or ammoxidation processes. The main characteristics of Bi-Mo mixed oxides utilized in these reactions are their abilities to use lattice oxygen to oxidize hydrocarbons and to be reoxidized in the presence of gaseous oxygen [1]. These catalysts can form several phases depending on the Bi/Mo ratio and reaction temperature [2]. The molecular structures of many of the phases constituting the bismuth molybdate systems are not completely known because of the difficulties encountered in determining the location of the oxygen atoms surrounding the metal sites by diffraction techniques. The $\text{Bi}_2\text{O}_3 \cdot n\text{MoO}_3$ phase with $n = 3$ is the α -form, that with $n = 2$ is the β -form and that with $n = 1$ is the γ -form. Of the various known bismuth molybdate phases, only the α -, β - and γ -phases are recognized as active catalysts for selective oxidation and ammoxidation. In order to understand the structure and its relationship to the observed catalytic activities, bismuth molybdate phases have been investigated using various techniques [3–8]. Despite their broadly similar catalytic performances, the α - and β -phases differ substantially in structure from the γ -phase. The structures of the α - and β -phases can be considered as defective fluorite structures, whereas the γ -phase is an Aurivillius-type structure [9].

The γ - Bi_2MoO_6 composition has been the subject of controversy due to its three-phase polymorphism [10]. The three polymorphs of γ - Bi_2MoO_6 are $\gamma(\text{L})$, $\gamma(\text{H})$ and $\gamma(\text{I})$. $\gamma(\text{L})$ - Bi_2MoO_6 is the low-temperature phase, in octahedral form, and $\gamma(\text{H})$ - Bi_2MoO_6 is the high-temperature phase, in tetrahedral form. Both $\gamma(\text{L})$ - Bi_2MoO_6 and $\gamma(\text{H})$ - Bi_2MoO_6 are stable whereas $\gamma(\text{I})$ - Bi_2MoO_6 is metastable and also is intermediate between them [10]. The $\gamma(\text{L})$ - Bi_2MoO_6 form is also known as ‘koechlinite’. The recent refinement of the $\gamma(\text{L})$ - Bi_2MoO_6 structure by means of neutron diffraction revealed that alternating layers of $\text{Bi}_2\text{O}_2^{2+}$ and MoO_4^{2-} are stacked perpendicular to the b -axis, and the structure is somewhat similar to the K_2NiF_4 structure [7]. The unit cell and qualitative structural features of $\gamma(\text{H})$ - Bi_2MoO_6 are well established. Recent x-ray powder and electron diffraction data indicated that the cation distribution in $\gamma(\text{H})$ - Bi_2MoO_6 forms a fluorite-related supercell with infinite channels of bismuth polyhedra surrounded by molybdenum tetrahedra [6]. Although the structure of the room temperature $\gamma(\text{L})$ - Bi_2MoO_6 phase and high-temperature $\gamma(\text{H})$ - Bi_2MoO_6 phase were described adequately, the nature of and dynamics involved in the phase transformation of the intermediate $\gamma(\text{I})$ - Bi_2MoO_6 phase was not investigated in detail because of its metastable nature. Although advanced techniques like *in situ* combined x-ray absorption spectroscopy and x-ray diffraction (XAS/XRD) [10], high-resolution neutron and synchrotron x-ray diffraction and transmission electron microscopy (TEM) [7] were utilized earlier in an effort to understand the phase transformations of γ - Bi_2MoO_6 , still there are several inconsistencies as regards detecting the nature and sequence of changes in the phase transformation, the transformation temperature, the transformation width, reversibility and the temperature ranges of existence of the phases.

On the basis of a thermodynamic model, Kodama and Watanabe [11] predicted that transformation from the $\gamma(\text{L})$ - Bi_2MoO_6 to the $\gamma(\text{I})$ - Bi_2MoO_6 form occurs reversibly at 570°C and that transformation from the $\gamma(\text{I})$ - Bi_2MoO_6 to the $\gamma(\text{H})$ - Bi_2MoO_6 phase occurs slowly and irreversibly at 604°C . The *in situ* combined XAS/XRD studies on the $\gamma(\text{L})$ - Bi_2MoO_6 composition indicated the transformation to the $\gamma(\text{I})$ - Bi_2MoO_6 phase at around 610°C and that to the $\gamma(\text{H})$ - Bi_2MoO_6 phase at 670°C [11]. Recently, Buttrey *et al* [7], on the basis of high-

resolution neutron powder diffraction, electron diffraction and synchrotron diffraction studies, reported the occurrence of reversible incommensurate-to-commensurate phase transformation to the γ (L)-Bi₂MoO₆ phase at around 567 °C preceding transformation to the irreversible γ (H)-Bi₂MoO₆ phase near 607 °C.

The reason for these inconsistencies might be the lack of a practical technique for following the transformation process dynamically, particularly as regards monitoring the change in coordination of the molybdenum with oxygen in each phase. Raman spectroscopy is one of the most convenient and powerful tools for unravelling details of the local and cooperative changes during transformations between phases. The primary advantage of Raman spectroscopy for solid-state structural transformation investigation over the x-ray technique is that while the latter is sensitive primarily to heavy ions, Raman spectroscopy is quite sensitive to the position and motion of light ions. Hardcastle and Wachs [8] reported Raman spectra of γ (L)-Bi₂MoO₆ and γ (H)-Bi₂MoO₆ at ambient conditions and introduced a systematic method for determining molecular structures of the molybdate species in these bismuth molybdate phases. However, the capability of Raman spectroscopy was not utilized to its full extent for probing the structural changes in the phase transformations of γ (L)-Bi₂MoO₆ phases during heating and cooling processes, dynamically. Thermo-Raman spectroscopy (TRS) in which Raman spectra are measured dynamically as a function of temperature has been applied successfully in the *in situ* investigation of solid-state phase transformations and composition changes [12–19]. The thermo-Raman technique has been utilized extensively in this work to derive further information on the phase transformations of γ (L)-Bi₂MoO₆.

2. Experimental details

2.1. Preparation of γ (L)-Bi₂MoO₆

The coprecipitation method was utilized to prepare the γ (L)-Bi₂MoO₆ phase [10]. Stoichiometric amounts of (NH₄)₆Mo₇O₂₄·4H₂O dissolved in (NH₄OH) and Bi(NO₃)₃·5H₂O dissolved in HNO₃ were introduced simultaneously into a beaker, with rapid stirring. The pH of the resulting solution was brought to 6–7 by the addition of ammonia. The resulting slurry was heated to boiling point and boiled dry, and the nitrate was then sublimed by heating at 425 °C for 4 h and the remaining mixture was calcined for 24 h at 525 °C. The calcined sample obtained was then gently washed with a diluted ammonia solution to remove the slight excess amount of MoO₃ present in the sample. The phase purity of the bright yellowish γ (L)-Bi₂MoO₆ powder obtained was confirmed by means of conventional powder x-ray diffraction (Shimadzu XD-5 diffractometer) patterns recorded using Cu K α radiation.

2.2. Thermo-Raman spectroscopy (TRS)

The experimental set-ups utilized for the thermo-Raman studies were described in detail earlier [12, 17]. The γ (L)-Bi₂MoO₆ powder sample was pressed into a shallow pit on a sample holder attached to a thermocouple in a home-made oven covered with glass. A programmable controller was used to control the temperature. The uncertainty in measuring the temperature was about 1 °C. Thermo-Raman spectra were measured using excitation by laser light of 50 mW power operating at a wavelength of 514.5 nm, from an argon-ion laser (Coherent, Innova 100-15). The scattered radiation was collected, analysed by a 0.5 m spectrophotometer (Spex) and detected by a CCD camera (Princeton Instruments, 1024 × 1024 pixels). Thermo-Raman spectra were taken continuously with suitable exposure times, such that each spectrum covered 1 °C in a dynamical thermal process.

To understand the nature of the phase transformation involved for the $\gamma(\text{L})\text{-Bi}_2\text{MoO}_6$ composition, the thermo-Raman spectra were collected following both heating and cooling thermal processes. The sample was heated from 25 to 570 °C at the rate of 5 °C min⁻¹ and retained at 570 °C for a period of 10 min. The sample was again heated from 570 to 720 °C at the rate of 1 °C min⁻¹ and then retained at 720 °C for 15 min, and then cooled down to a temperature of 25 °C at the rate of 5 °C min⁻¹.

In an effort to gain an understanding of the reversibility, the $\gamma(\text{L})\text{-Bi}_2\text{MoO}_6$ sample was heated up to 640 °C at the rate of 5 °C min⁻¹ and then thermo-Raman spectra were collected while cooling the sample from 640 to 25 °C at the rate of 5 °C min⁻¹.

3. Results and discussion

The room temperature $\gamma(\text{L})\text{-Bi}_2\text{MoO}_6$ phase was studied earlier by means of x-ray diffraction [10] and neutron diffraction [7]. Buttrey *et al* [7] reported that the structure of $\gamma(\text{L})\text{-Bi}_2\text{MoO}_6$ was found to consist of alternating layers of $\text{Bi}_2\text{O}_2^{2+}$ and MoO_4^{2-} . They also mentioned that the molybdenum has distorted octahedral coordination with four equatorial oxygen sites, involving two longer and two shorter equatorial bonds and two closer apical oxygen sites. The distorted MoO_6 octahedra share corners along *a* and *c* to form an infinite $(\text{MoO}_4)_n$ layer [7].

The site symmetry approach in Raman spectroscopy proved to be an effective tool in the characterization of the structure of transition metal oxides. For metal oxides with distorted molecular geometries, however, the site symmetry approach cannot be a reliable technique. Hence in this work the recently developed Hardcastle empirical correlation method has been utilized for the interpretation and assignment of the Raman spectrum of $\gamma(\text{L})\text{-Bi}_2\text{MoO}_6$ [8].

In general, Raman bands observed above 600 cm⁻¹ for $\gamma(\text{L})\text{-Bi}_2\text{MoO}_6$ were assigned to Mo–O stretches and those below 400 cm⁻¹ were assigned to bending, wagging and external modes by directly correlating the Mo–O bond lengths [8]. The MoO_6 coordination environment of $\gamma(\text{L})\text{-Bi}_2\text{MoO}_6$ at 300 K depicted by Buttrey *et al* [7] using neutron diffraction data clearly revealed the Mo polyhedron to consist of four short Mo–O bonds plus two much longer Mo–O bonds. According to the Hardcastle criterion, the relation between the Raman stretching frequency (wavenumber) and the corresponding Pauling strength of a Mo–O bond (valence unit) can be expressed as $S_{\text{Mo-O}} = [0.256 \ln(32\,895/\nu)]^{-6}$ [8]. The Raman bands observed at 854, 793, 715 and 404 cm⁻¹ for $\gamma(\text{L})\text{-Bi}_2\text{MoO}_6$ measured at 25 °C (figure 1) were assigned to Mo–O stretching modes of the distorted MoO_6 octahedra [8]. The spectral variation observed in the thermo-Raman spectra in the temperature intervals from 25 to 225 and 290 to 370 °C are shown in figure 1. The Raman spectrum observed at 25 °C shows a very strong band at 793 cm⁻¹ along with two shoulder bands at 814 and 789 cm⁻¹. In addition to these, bands with medium intensity at 854, 715, 358 and 286 cm⁻¹ were also seen. As the temperature increased, the strong band at 793 cm⁻¹ was found to broaden; there was also a slight shift in the positions to 796 cm⁻¹. The medium-intensity bands were also broadened and also shifted in position from 854, 358 and 286 to 847, 352 and 282 cm⁻¹, respectively, at around 250 °C. The thermo-Raman spectra observed in the temperature interval from 250 to 300 °C revealed no major spectral variations. However, the thermo-Raman spectra collected in the temperature interval from 310 to 615 °C indicate appreciable decrease in intensity, shift in position and broadening of the Raman bands.

The absence of significant spectral variation in the thermo-Raman spectra collected in the temperature interval from 25 to 610 °C revealed that the skeleton structure of the $\gamma(\text{L})\text{-Bi}_2\text{MoO}_6$ phase was not dramatically disturbed in this temperature range. However, the observation of minute changes, such as the disappearance of the triplet nature of the dominant Mo–O stretching

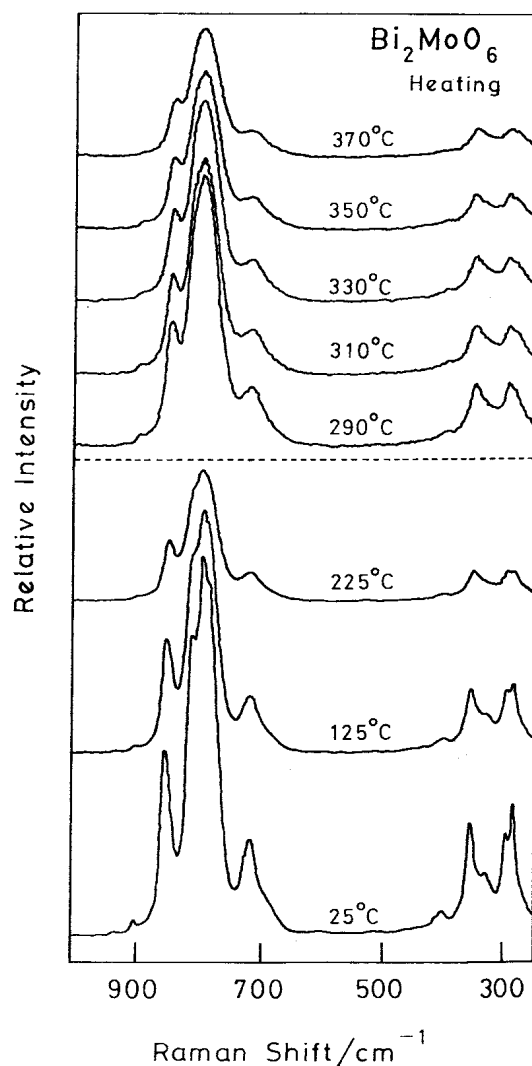


Figure 1. Thermo-Raman spectra of the γ (L)- Bi_2MoO_6 phase measured in the two temperature intervals from 25 to 225 °C and 290 to 370 °C during the heating process.

bands at around 793 cm^{-1} and the decrease in intensity, shift in position and broadening of the remaining Raman bands, suggested that there might be some subtle rearrangements in the crystal structure.

From the Mo–O stretching modes observed in the room temperature Raman spectrum of the γ (L)- Bi_2MoO_6 phase, three short Mo–O bonds with lengths 1.761, 1.797 and 1.847 Å and one long Mo–O bond with length 2.222 Å were recognized using the Hardcastle relation [8]. However, one more short and one more long Mo–O bond distance were not derived due to the very weak natures of their corresponding bands. The thermal evolution of the Mo–O distances derived using the Hardcastle relation is shown in figure 2. One of the shorter Mo–O (apical) bonds exhibits a gradual decrease in bond length upon heating from room temperature and an appreciable decrease in the bond length in the temperature interval from

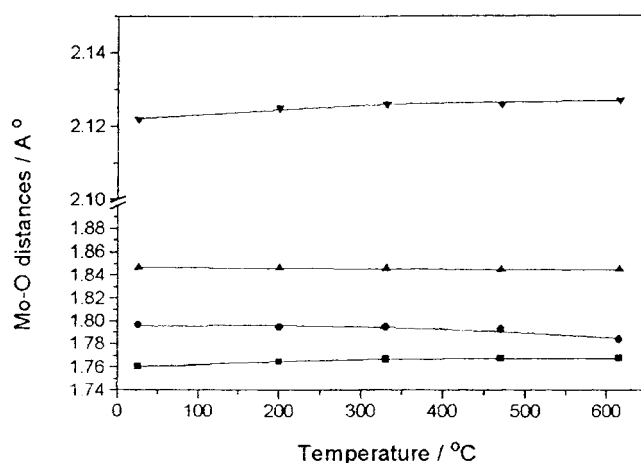


Figure 2. Thermal evolution of Mo–O bond distances in distorted MoO₆ octahedra of the γ (L)-Bi₂MoO₆ phase.

310 to 610 °C. However, of the remaining two shorter Mo–O (equatorial) bonds, one showed a gradual increase and the other showed a decrease in the bond length in the temperature interval from room temperature to 610 °C. The observation of the gradual increase and decrease in the bond lengths of the shorter equatorial Mo–O bonds upon heating and an appreciable decrease in the bond length of the apical Mo–O distance from 310 °C strongly suggested a gradual anisotropic thermal expansion of the unit-cell parameters as the initial modification and further appreciable distortions in the MoO₆ octahedra structure. Although the variation of the Mo–O distances as a function of temperature and spectral variation in the thermo-Raman spectra in this temperature interval indicated the possibility of transformations to the intermediate phase, there is no strong evidence for a change of coordination during this transformation.

The spectra collected in the temperature range from 615 to 665 °C shown in figure 3 show three major spectral variations. The first major spectral variation was the appearance of a band at 890 cm⁻¹ from 620 °C onwards. The intensity of this band increases with further increase of temperature and it is a very sharp and strong band at around 655 °C. The second major spectral variation was a steady decrease in intensity of the medium-intensity band at 847 cm⁻¹ from 625 °C onwards and then a split into two weak bands at 814 and 775 cm⁻¹ at around 655 °C. The third major spectral variation arises from the bands at 352 and 282 cm⁻¹. They showed decreases in their intensity from 615 to 645 °C and then appeared as a broad bands centred at 312 cm⁻¹. However, with further increase of temperature up to 720 °C no dramatic variations in the spectral profile were observed.

The spectral variation shown in figure 3 for the transformations to γ (H)-Bi₂MoO₆: indicated that the transformation is manifested as a gradual modification in the Raman spectra starting at around 620 °C and ending at 660 °C; revealed the sluggish nature of the transformations; and also clearly indicated transformation from highly distorted MoO₆ octahedra to a new structure. In contrast to the strong antisymmetric stretching Mo–O mode observed at 793 cm⁻¹ for the distorted MoO₆ octahedra in the γ (L)-Bi₂MoO₆ phase, the Raman spectrum measured at 665 °C showed a strong antisymmetric stretching Mo–O mode at 890 cm⁻¹, which is characteristic of MoO₄ tetrahedra. The absence of Mo–O stretching bands in the 730–540 cm⁻¹ region of the spectrum measured at 665 °C argues against the presence of MoO₆ octahedra as well as bridged MoO₅ and MoO₄ species. The presence of

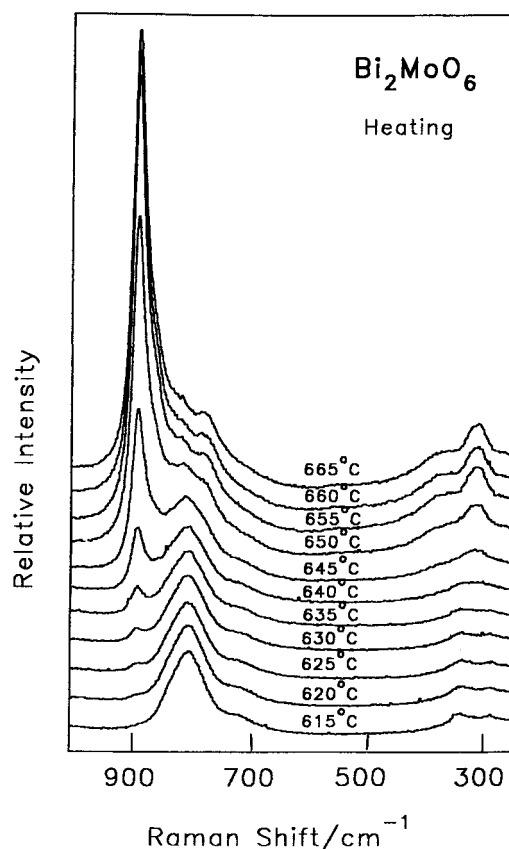


Figure 3. Thermo-Raman spectra measured during the heating process in the temperature interval from 615 to 665 °C for the transformation to $\gamma(\text{H})\text{-Bi}_2\text{MoO}_6$.

slightly distorted MoO_4 in $\text{Na}_2\text{MoO}_4 \cdot 2\text{H}_2\text{O}$ and $\text{Bi}(\text{FeO}_4)(\text{MoO}_4)_2$ indicated a Raman Mo–O stretching band at around 897 cm^{-1} [20, 21]. The above observations strongly indicate that the $\gamma(\text{H})\text{-Bi}_2\text{MoO}_6$ structure contains slightly distorted and isolated MoO_4 tetrahedra and this is in agreement with recent high-resolution neutron diffraction data [7].

The Raman spectrum profiles of $\gamma(\text{H})\text{-Bi}_2\text{MoO}_6$ measured at 720 and 25 °C in the cooling process are shown in figure 4. The spectral variations observed in the temperature interval from 720 to 25 °C during the cooling process revealed no major changes in the spectral profile. However, close observation of the spectral variation in the cooling process indicated a shift in the position of the Mo–O stretching bands to higher wavenumber, increases in intensities of all the bands and reductions in the bandwidths of the dominant bands. The reason for the above observations might be the thermal effect at higher temperature. The thermo-Raman spectra measured at 720 and at 25 °C (magnified 20 times) shown in figure 4 clearly revealed a shift in the band position of the Mo–O stretching band from 890 cm^{-1} at 720 °C to 900 cm^{-1} at 25 °C. The spectrum measured at 25 °C also showed bands with medium-to-strong intensity at 867 and 825 cm^{-1} and medium intensity at 882, 791 and 773 cm^{-1} .

Recent high-resolution neutron diffraction studies indicate that $\gamma(\text{H})\text{-Bi}_2\text{MoO}_6$ and $\beta\text{-Bi}_2\text{Mo}_2\text{O}_9$ structures have strikingly similar features—not only sharing common fluorite cation rearrangements, but also having similarities in channel structure, site potentials, valence sums

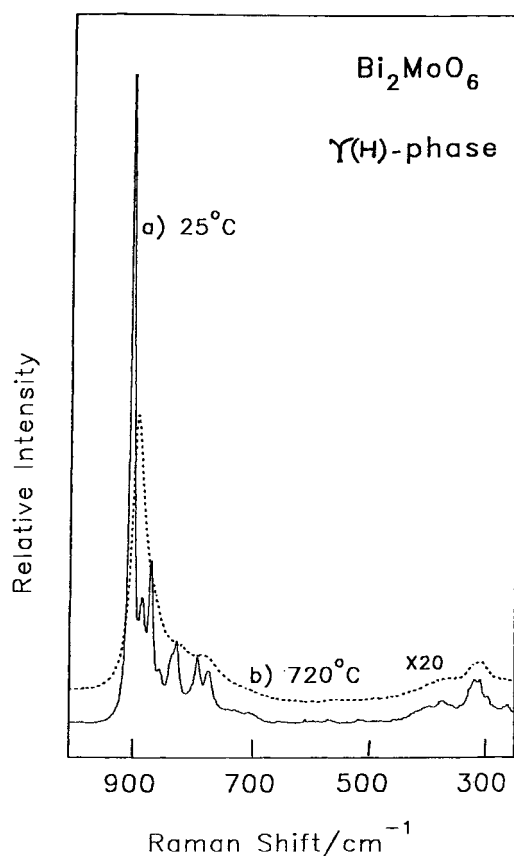


Figure 4. Comparison of the Raman spectra of the $\gamma(\text{H})$ - Bi_2MoO_6 phase measured (trace a) at 25 °C after cooling and (trace b) at 720 °C.

and lone pair orientation [7]. Hence the Raman spectrum measured at 720 °C in this work corresponding to the $\gamma(\text{H})$ - Bi_2MoO_6 phase at high temperature resembles those for the β - $\text{Bi}_2\text{Mo}_2\text{O}_9$ phase presented by Hardcastle and Wachs [8]. The similarity of the spectral profile of the $\gamma(\text{H})$ - Bi_2MoO_6 phase measured at 720 °C and that measured after cooling down to 25 °C in figure 4 rules out the possibility of the formation of β -phase structure consisting of Mo^{6+} in tetrahedra coordination at high temperature [22].

The spectral variation observed in the thermo-Raman spectra collected while cooling the sample from 640 °C (the $\gamma(\text{L})$ - Bi_2MoO_6 sample had been heated up to 640 °C at the rate of 5 °C min^{-1}) to 25 °C at the rate of 5 °C min^{-1} is shown in figure 5. As the cooling started from 640 °C the band at 890 cm^{-1} showed an increase in intensity and then appeared as a strong band with a slight shift in the band position to 899 cm^{-1} at 25 °C. The very weak band observed at 705 cm^{-1} in the temperature region of 640 °C also showed a sharp increase in intensity and then appeared as a band of medium intensity with a new band position at 715 cm^{-1} at 25 °C. Similarly the intensities of the bands corresponding to the $\gamma(\text{L})$ - Bi_2MoO_6 phase also increased and then they appeared as bands of medium and weak intensities at 25 °C. Earlier reports indicated that the transformation to the $\gamma(\text{I})$ - Bi_2MoO_6 phase is reversible, while the transformation to the $\gamma(\text{H})$ - Bi_2MoO_6 phase is irreversible [10]. The spectral variation (figure 5) observed in the thermo-Raman spectra collected during the transformation of the phase at the

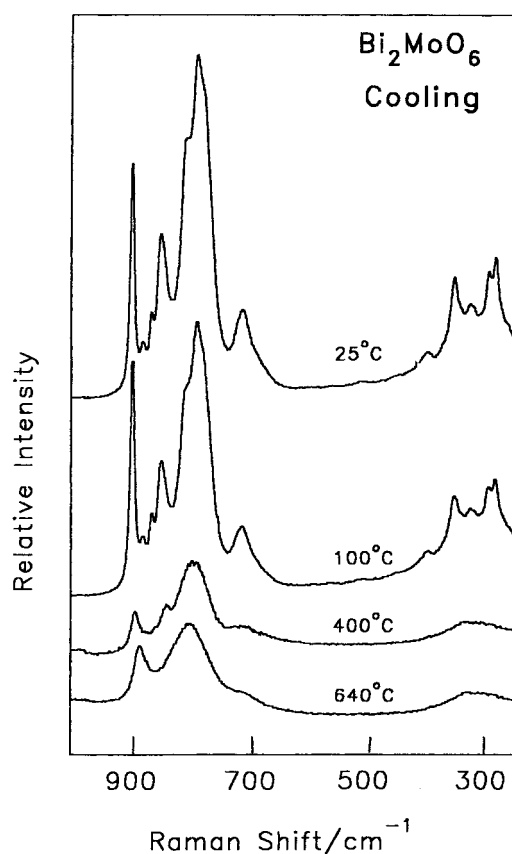


Figure 5. Thermo-Raman spectra (for the $\gamma(\text{L})$ - Bi_2MoO_6 sample that had been heated up to 640 °C) measured in the temperature interval from 640 to 25 °C during the cooling process.

verge of becoming a $\gamma(\text{H})$ - Bi_2MoO_6 phase, i.e. going from highly distorted MoO_6 octahedral to distorted MoO_4 tetrahedral coordination, clearly indicated reversibility of the transformation to the Bi_2MoO_6 phase, with a mixture of distorted MoO_6 octahedral and MoO_4 tetrahedral coordination.

4. Conclusions

In this work, detailed thermo-Raman studies have been carried out on $\gamma(\text{L})$ - Bi_2MoO_6 in an effort to gain an understanding of the structural evolution and phase transformation involved during a dynamical thermal process. The spectral variations, shifts in band positions, decreases in intensities and broadenings of Mo–O modes observed in the thermo-Raman spectra and thermal evolution of the Mo–O bonds in the temperature interval from 25 to 610 °C strongly suggest that the transformation from the $\gamma(\text{L})$ - Bi_2MoO_6 to the $\gamma(\text{I})$ - Bi_2MoO_6 phase involves a gradual anisotropic thermal response of Mo–O bonds initially, upon heating, and further appreciable increase in the octahedral distortion from 310 °C onwards, until the phase is on the verge of becoming composed of distorted tetrahedra. Although the thermal evolution of the oxygen bond distances and the thermo-Raman spectral variation provided evidence for the existence of an intermediate $\gamma(\text{I})$ - Bi_2MoO_6 phase, there is no strong support for coordination

change. The absence of significant spectral variations revealed that the skeleton structure of the intermediate $\gamma(\text{I})\text{-Bi}_2\text{MoO}_6$ phase resembles more that of the $\gamma(\text{L})\text{-Bi}_2\text{MoO}_6$ phase.

The spectral variation in the thermo-Raman spectra observed for the transformations to $\gamma(\text{H})\text{-Bi}_2\text{MoO}_6$ starting at around 620 °C and ending at 660 °C revealed the sluggish nature of the transformations and also clearly indicated transformation from highly distorted MoO_6 octahedra to distorted tetrahedra. The comparison of the spectrum measured at 720 °C with that measured after cooling down to 25 °C in this work clearly rules out the possibility of the formation of a $\beta\text{-Bi}_2\text{Mo}_2\text{O}_9$ phase structure consisting of Mo^{6+} in tetrahedral coordination at high temperature. The thermo-Raman spectra collected during the transformation of the phase on the verge of becoming a $\gamma(\text{H})\text{-Bi}_2\text{MoO}_6$ phase, i.e. going from highly distorted MoO_6 octahedral to distorted MoO_4 tetrahedral coordination, clearly indicated reversibility in the transformation to the Bi_2MoO_6 phase, with a mixture of distorted MoO_6 octahedral and MoO_4 tetrahedral coordination. The initial anisotropic thermal response of the Mo–O bonds and further appreciable distortions in the MoO_6 octahedra caused by decrease in the bond length of the apical Mo–O distance in the temperature interval from 310 to 610 °C lead to charge transfer between $[\text{Bi}_2\text{O}_2]^{2+}$ and $[\text{MoO}_4]^{2-}$ layers, and this interlayer charge transfer may be a factor contributing to the catalytic performance of this material.

Acknowledgment

The authors are grateful to Professor Hua Chang, Department of Chemistry, NTHU, Taiwan, ROC, for providing the thermo-Raman facilities.

References

- [1] Aykan K 1968 *J. Catal.* **12** 281
- [2] Galvan D H, Fuentes S, Avalos-Borja M and Cota-Araiza L 1993 *Catal. Lett.* **18** 273
- [3] Chen H Y and Sleight A W 1986 *J. Solid State Chem.* **63** 70
- [4] Wuzong Z, Jefferson D A, Alario-Franco M and Thomas J M 1987 *J. Phys. Chem.* **91** 512
- [5] Watanabe A, Horiuchi S and Kodama H 1987 *J. Solid State Chem.* **67** 333
- [6] Buttrey D J, Vogt T, Wildgruber U and Robinson W R 1994 *J. Solid State Chem.* **111** 118
- [7] Buttrey D J, Vogt T and White B D 2000 *J. Solid State Chem.* **155** 206
- [8] Hardcastle F D and Wachs I E 1991 *J. Phys. Chem.* **95** 10 763
- [9] Reilly L M, Sankar G and Catlow C R A 1999 *J. Solid State Chem.* **148** 178
- [10] Sankar G, Roberts M A, Thomas J M, Kulkarni G U, Rangavittal N and Rao C N R 1995 *J. Solid State Chem.* **119** 210
- [11] Kodama H and Watanabe A 1985 *J. Solid State Chem.* **56** 225
- [12] Chang H and Huang P J 1997 *Anal. Chem.* **69** 1485
- [13] Murugan R, Ghule A and Chang H 1999 *J. Appl. Phys.* **86** 6779
- [14] Murugan R, Huang P J, Ghule A and Chang H 2000 *Thermochim. Acta* **346** 83
- [15] Murugan R, Ghule A and Chang H 2000 *J. Phys.: Condens. Matter* **12** 677
- [16] Murugan R, Ghule A, Bhongale C and Chang H 2000 *J. Mater. Chem.* **10** 2157
- [17] Chang H, Murugan and Ghule A 2001 *Thermochim. Acta* **374** 45
- [18] Murugan R and Chang H 2001 *J. Chem. Soc. Dalton Trans.* **3125**
- [19] Ghule A, Murugan R and Chang H 2001 *Inorg. Chem.* **40** 5917
- [20] Mahadevan Pillai V P, Pradeep T, Bushiri M J, Jayasree R S and Nayar V U 1997 *Spectrochim. Acta* **53** 867
- [21] Maczka M, Kojima S and Hanuza J 2000 *J. Phys. Chem. Solids* **61** 735
- [22] Antonio M R, Raymond G, Teller, Sandstrom D R, Mehicic M and Brazdil J F 1988 *J. Phys. Chem.* **92** 2939